Observation and Modeling of the Structure of Premixed Turbulent Propagating Flames

H.Kido, S.W.Huang and K.Nakashima

Faculty of Engineering
Kyushu University
6-10-1, Hakozaki
Higashi-ku, Fukuoka 812
Japan

ABSTRACT

The structure of premixed turbulent flames in a constant volume vessel was investigated using a micro-probe method that was developed in this work(1). The experimental results suggest the existence of "reactant-islands" and the flame structure changing from a wrinkling pattern at low u'/S_{L0} ratios to an islands-like one at high u'/S_{L0} ratios, where u' is the turbulence intensity and S_{L0} is the laminar burning velocity. Based on the experimental results, a model for the flame structure has been developed, where a turbulent flame was separated into two parts: a wrinkled flame front and some island flamelets behind it. The fractions of them were supposed to change continuously according to a proposed function of u'/S_{L0}. The model provides the turbulent burning velocity, S_T, a characteristic time and a characteristic thickness for turbulent flames, and was examined by comparing the predicted S_T/S_{L0} ratios with the measured ones.

INTRODUCTION

Experimental studies on the turbulent flame structure may be divided into two aspects: the local structure of the flamelets and the whole geometry of them.

Experimental evidence shows that reaction in premixed turbulent flames at low to moderate turbulence intensities is confined to thin flamelets (1-3). In fact, for premixed propagating flames at high as to the ratio of u'/S_{L0} being of order 10, the electric potential signals detected from them showed sharp spikes similar to those from premixed laminar flames(1), implying that thin flamelets remain in the flame even at rather high turbulence intensities.

Many of the geometric properties of the flame surfaces have been clarified recently by the schlieren photography(4,5), micro-probe method(1), and particularly, by the laser tomography(6,7). Obtained by the laser tomography, two-dimensional images of turbulent flames show that the turbulent flame surfaces have fractal properties(7,8).

The fact that the turbulent flame surfaces have fractal properties receives more and more attention in recent theoretical studies. The first model based on the fractal properties of turbulent flame surfaces, for calculating S_T/S_{L0} ratios, has been made by Gouldin(9). But, in Gouldin's model, no details were given on how to deal with the flamelets separated from the flame front(6-8).

In this work, the experiments were focused on how the turbulent flame structure changes with the u'/S_{L0} ratio. Based on the experimental results, the modeling work was focused on: (a) how to describe the flame structure changing from a wrinkling pattern at low u'/S_{L0} ratios to an islands-like one at high u'/S_{L0} ratios quantitatively? (b) how to calculate the turbulent burning velocity with the flame structure model? (c) how to define a characteristic time for a turbulent flame, which is analogous to the transition time, $2\delta_{L0}/S_{L0}$, for a laminar flame, where δ_{L0} is the laminar flame reaction zone thickness.

EXPERIMENTAL APPARATUS AND MIXTURES

Combustion Chamber and Turbulence Field

The combustion chamber used in this experiment was a constant-volume vessel having a ball-like inner space(1). An ignition plug was located at the center of the chamber. The turbulence field created by four fans cooperating with four perforated plates surrounding the inner space was steady and approximately isotropic. The turbulence intensity was controlled by the fan speed. The characteristics of the turbulence field had been measured and reported in reference (10). Some of the results are given in Fig.1, where L_f is the longitudinal integral length scale, and η_K is the Kolmogorov length scale for air.

Micro-Probe and Measurement Circuit

A micro-probe method called flame-potential probe method was developed and used in this work. The method is similar to the Langmuir probe method, but the probe works on a different

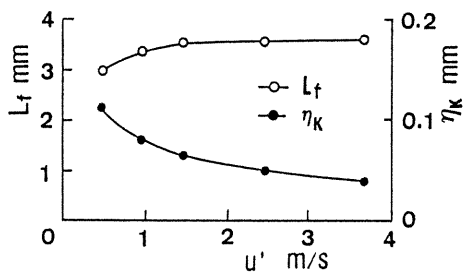

Fig.1 Characteristics of the turbulence field in the combustion chamber

Table 1 Properties of mixtures used

MIXTURE	MOLAR FRACTION				Φ	S_{LO}	δ_{LO}	η_0	T_b	$\nu\times10^5$
	C_3H_8	O_2	N_2	He		m/s	mm	mm	K	m^2/s
85-P10-14	1.0	5.0	12.0	2.00	1.0	.858	.146	.0284	2496	1.517
85-P10-18	1.0	5.0	11.0	4.50	1.0	.846	.177	.0365	2472	1.715
79-P10-21	1.0	5.0	10.5	6.50	1.0	.791	.213	.0454	2440	1.880
49-P10-20	1.0	5.0	17.0	0.36	1.0	.494	.198	.0415	2329	1.411
50-P10-22	1.0	5.0	16.5	2.00	1.0	.501	.219	.0476	2310	1.511
49-P10-24	1.0	5.0	16.0	3.20	1.0	.493	.240	.0534	2299	1.587
46-P10-29	1.0	5.0	15.4	5.60	1.0	.464	.289	.0675	2262	1.741
33-P10-30	1.0	5.0	20.0	2.00	1.0	.331	.298	.0712	2168	1.508
22-P10-36	1.0	5.0	24.0	0.00	1.0	.224	.358	.0898	2060	1.411
17-P10-45	1.0	5.0	26.0	0.00	1.0	.169	.451	.1190	1986	1.415

principle and was shown to have higher spatial resolution. The probes as shown in Fig.2 were inserted into the chamber through the window. Both of them have the same sizes of 0.2mm in diameter and 0.6mm in length. They were at first used to demonstrate the difference in spatial resolution between the Langmuir probe method and the flame-potential probe method, and then used for the real measurement as flame-potential probes.

There are two circuits shown in Fig.2, where circuit I was used for the real measurements, and circuit II is a typical one for the Langmuir probe method and was used to obtain the ion current signal for comparison. In the circuits, R_{in} is the input impedance of the signal recording device; R_1 and R_2 are variable resistances, usually being set infinite to increase the S/N ratio.

Mixtures

There were ten propane/air mixtures used in the experiment, whose compositions are given in Table 1, where S_{LO} is the laminar burning velocity; δ_{LO} is the thickness of laminar flame reaction zone; Φ is the equivalence ratio; η_0 is the thickness of laminar flame preheat zone; ν is the kinematic viscosity; and T_b is the constant-pressure adiabatic flame temperature, of the mixture. In order to control the laminar burning velocity and the laminar flame thickness, artificial air was used.

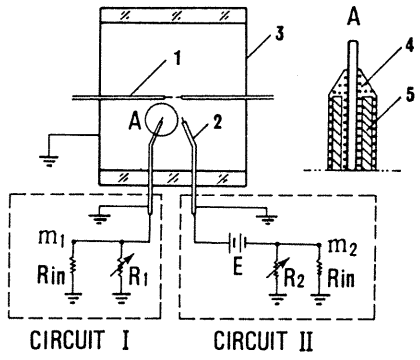

Fig.2 Measurement circuits and probe
1-Ignition plug; 2-Probe; 3-Combustion chamber; 4-Insulator; 5-Supporting tube

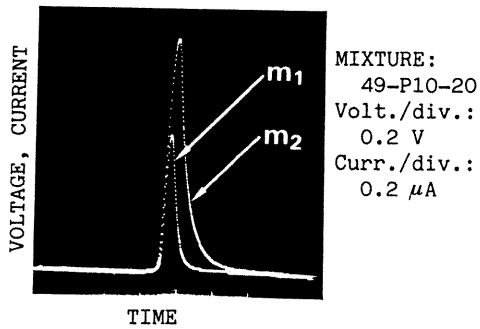

Fig.3 Flame potential signal and ion current signal from the same laminar flame

MICRO-PROBE METHOD AND RESULTS

Principle

As the principle of the flame-potential probe method has been reported in reference (1), here we only indicate: (a) A flame-potential probe is similar to a Langmuir probe in construction as shown in Fig.2; (b) It detects a flamelet by the electric potential signal instead of the ion current signal of the flamelet; (c) It has a higher spatial resolution than a Langmuir probe as shown in Fig.3, where m_1 was obtained by a flame-potential probe and m_2, by a Langmuir probe; (d) It is necessary to insulate any conductor from the flame except the sensor of the probe; (e) Compared with the Langmuir probe, it has little electrical influence on the flame structure.

Typical Flame Potential Signals and Number of Flamelets in the Flame Zone

Typical flame potential signals are shown in Fig.4, which were detected by a probe located at 25mm away from the chamber center, from the premixed propagating turbulent flame of mixture 49-P10-20, at a turbulence intensity of 2.45m/s.

For a premixed propagating laminar flame, there is only one spike shown in its flame potential signal since only one flamelet passed through the probe. The fact that, from a turbulent flame, more than one spike were detected as shown in Fig.4, was interpreted as that more than one flamelet existed in the turbulent flame zone as each spike in the signal can be identified with a flamelet passing through the probe. The same fact might also be attributed to more than one time a single flamelet passing through the probe, but this is unlikely because the flame propagation speed was much faster than the turbulence fluctuation speed. As many of the signals showed three or more spikes, particularly in the case of high turbulence intensities, it is concluded that this result suggests the existence of islands-like flamelets in the turbulent flame zone. Some of the measurement results of the number of spikes from flames with different turbulence intensities are

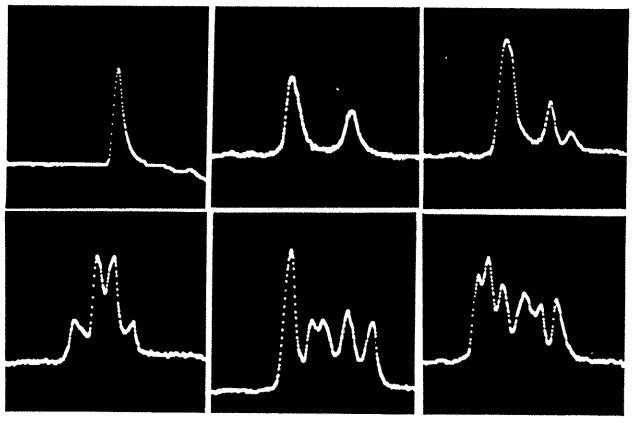

Fig.4 Typical flame potential signals from a turbulent flame

given in Fig.5, showing that the number of flamelets in the turbulent flame zone increases with increasing the u'/S_{L0} ratio.

Turbulent Flame Zone Thickness

So far the definition for turbulent flame zone is ambiguous, partially owing to the fact that the turbulent flame structure is still not well understood. At the present case, we define the turbulent flame zone as the space in which flamelets exist, and the thickness of the zone as the distance from the front edge of the first flamelet to the rear edge of the last one. When measured by a micro-probe, the flame zone thickness was identified with the spatial distance corresponding to the duration of Δt as shown in Fig.6.

In order to measure the flame zone thickness, three methods including the so-called constant flame propagation speed method, double-probe method and graphic method, have been used(1).

The results shown in Fig.7 were obtained by the double-probe method, where $P(d_T \leq X)$ represents the probability of the flame zone thickness, d_T, being not greater than X, and pdf is the probability density function. It is shown that the flame zone thickness increases with increasing the u'/S_{L0} ratio.

Average Flamelet Separation

The term "average flamelet separation" (abbreviated to AFS) refers to the average separation distance between two successive flamelets in the flame zone. It was obtained from the average duration between two successive spikes in the flame potential signal and the separation distance of two probes in a way as shown in Fig.8. When the first spike in signal b occurred at the time close to that of the ith spike in signal a, the AFS value was estimated by:

$$AFS = \frac{X(t_{i,a} - t_{1,a})}{(i-1)(t_{1,b} - t_{1,a})} \qquad (1)$$

where X is the separation of the two probes. But, any data not satisfying $|t_{i,a} - t_{1,b}| \ll (t_{1,b} - t_{1,a})$ were abandoned.

The AFS values obtained in this way for three mixtures at various turbulence intensities are given in Table 2, where σ is the standard deviation from AFS, the Damkohler numbers Da_η and Da_δ as well as Reynolds number Re were defined as

$$Da_\eta = L_f S_{L0} / (4u'\eta_0) \ , \quad Da_\delta = L_f S_{L0} / (4u'\delta_{L0}) \ , \qquad (2)$$

$$Re = u' L_f / \nu \ . \qquad (3)$$

From the table, one can see that all of the AFS values are about two times the turbulence longitudinal integral length scale, L_f.

The AFS value is a characteristic of the flame structure and was regarded as some quantity relative to the mean size of initially generated reactant-islands(1).

Combustion Regimes

One of the ways to describe the structure of various turbulent flames is to sort the flames into different combustion regimes in a Re -Da plane(11) or a u'/S_{L0} -L_f/η_0 plane(12) according to

Table 2 Average Flamelet Separation

MIXTURE	u'	L_f	Re	Da_η	Da_δ	AFS	σ
	m/s	mm				mm	mm
46-P10-29	1.58	3.55	322	3.86	0.90	5.3	1.5
79-P10-21	3.67	3.60	703	4.27	0.91	6.6	2.1
49-P10-20	2.14	3.56	540	4.95	1.03	5.8	1.8
46-P10-29	2.66	3.56	550	2.30	0.54	6.9	2.5
79-P10-21	2.88	3.57	544	5.40	1.15	6.2	2.2

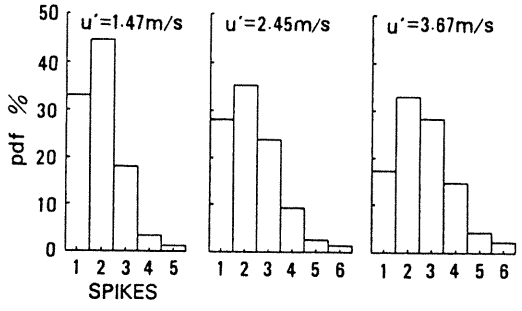

Fig.5 Number of flamelets in the flame zone (Mixture 49-P10-20)

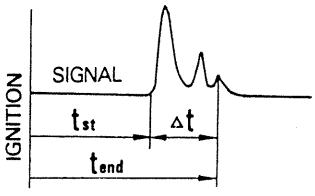

Fig.6 Definition of flame zone thickness

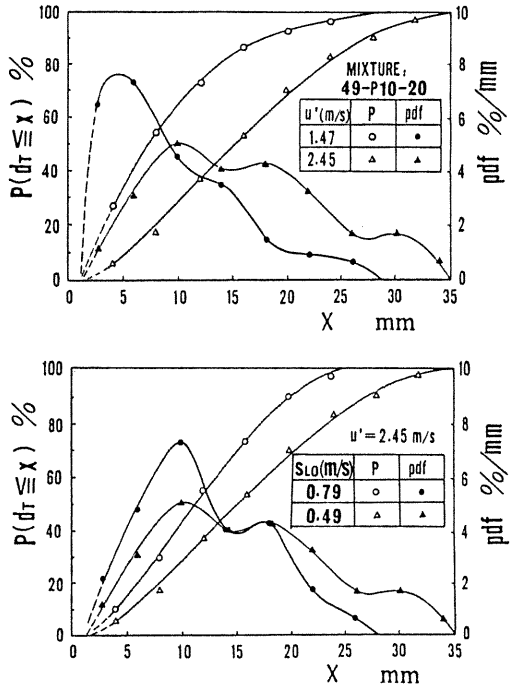

Fig.7 Distribution and pdf of turbulent flame zone thickness

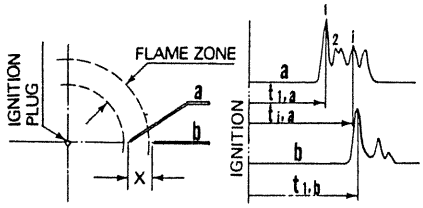

Fig.8 Measurement of flamelet separation

some critical conditions such as Da =1, $u'/S_{L0}=1$, $\eta_0/\eta_K=1$, etc. Indeed, these conditions have obvious physical meanings, but it is preferred that the flame structure be described in a geometrical way if possible.

In a previous work(13), the authors proposed a simple combustion regime model, making an attempt to describe the flame structure in a geometrical way. According to the model, the premixed turbulent propagating flames are sorted into three regimes. In regime I, the flame is supposed to have a single continuous wrinkled flamelet because of low turbulence intensities; In regime II, some island flamelets behind the flame front are generated because of high turbulence intensities; And, in regime III, the turbulence intensities are so high that some flamelets begin to extinguish locally owing to high strain rates.

In this work, an attempt was made to identify the boundary between regime I and regime II using the micro-probe method. The identification of the boundary between regime II and III can be expected to be done by laser tomography or other techniques.

According to the definition of regime II, when a flame in regime II is observed using a micro-probe, some of the obtained signals should show three or more spikes. If such signals are not found among a number of samples, the flame should belong to regime I. As a turbulent flame can show three or more spikes in its flame potential signal even in regime I owing to a corrugated flame front, the critical turbulence intensity, only above which can a signal have three or more spikes, is the lowest turbulence intensity of the boundary between regime I and II. Such critical turbulence intensities for ten mixtures have been determined in this work and are shown in Fig.9 with solid circles. The boundary determined in this way is in fact the one between "two spikes" and "three spikes or more". At the real boundary between regime I and II, the critical u' values are expected to be higher than but close to these u' values. In a similar way, the critical u' values at the boundary between "single spike" and "two spikes or more" were also determined and are shown in Fig.9 with open circles.

MODELING OF THE TURBULENT FLAME STRUCTURE

Assumptions

1. In the turbulent flame zone there exist a wrinkled continuous flame front and some separated island flamelets. The mixture in a unit volume in the flame zone, consumed by the island flamelets within their characteristic time, τ_D, is f_D, and that by the wrinkled flame front within its characteristic time, τ_C, is fw. By definition, $\tau_C=2\delta_{L0}/S_{L0}$, where δ_{L0} is the laminar flame thickness, and $\tau_D=Xc/(2Sc)$, where Xc is the mean size of the initially separated reactant-islands, assumed as L_f, and Sc is the burning velocity in the radial direction of the island. f_D is assumed to take the form of

$$f_D=\exp(-CS_{L0}/u'), \tag{4}$$

thus,

$$fw=1-f_D, \tag{5}$$

where C is a constant greater than zero.

2. The flamelets are strained by the eddies with the Taylor microscale λ_g, and the local laminar burning velocity S_L can be estimated by a formula proposed by Law(9). When the lewis number of the deficient reactant species is unity for stoichiometric mixtures, it is reduced to

$$S_L=S_{L0}(1-Ka) \tag{6}$$

where Ka is the Karlovitz number. By definition,

$$Ka=\gamma\nu/(PrS_{L0}^2) \tag{7}$$

where Pr is the Prandtl number; $\gamma=u'/\lambda_g$ is the strain rate; ν is the kinematic viscosity of the mixture. Both ν and λ_g were estimated at the temperature of the unburned mixture in this work.

3. The preheat zone of the flamelets is thickened by the Kolmogorov vortices and the thickness of the thickened preheat zone, η, can be estimated by

$$\eta=\eta_0+C_1 v_K(\eta_0/S_{L0}) \tag{8}$$

where C_1 is a constant of order one, v_K is the Kolmogorov velocity scale, and η_0/S_{L0} is the transition time of the preheat zone. η is called locally thickened preheat zone thickness.

4. All flame surfaces involved in a turbulent flame are fractal surfaces with an outer cutoff, ϵ_0, being equal to L_f, and an inner cutoff, ϵ_i, being determined by the Kolmogorov length scale, η_K, as well as the locally thickened preheat zone thickness, η, in the following way.

$$\epsilon_i=(\eta_K^2+\eta^2)/(\eta_K+\eta) \tag{9}$$

This is because the value of η_K becomes

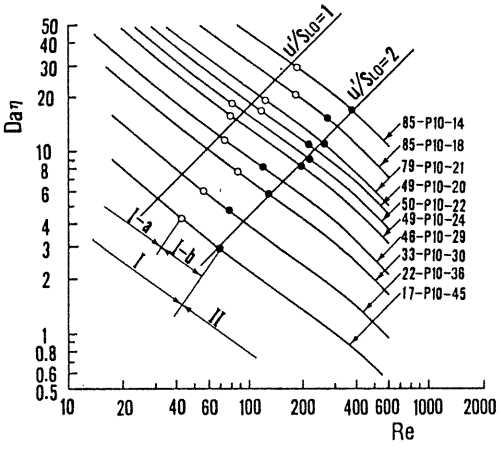

Fig.9 Combustion regimes

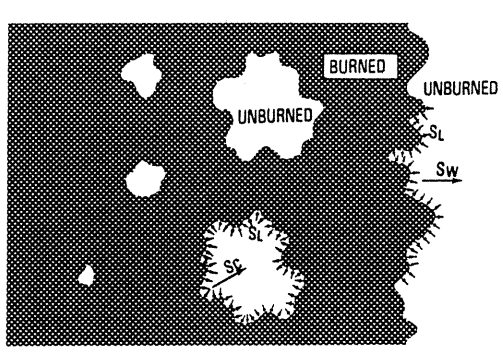

Fig.10 Wrinkled flame burning velocity and local laminar burning velocity

smaller than that of η at high turbulence intensities, and the inner cutoff is presumed to be influenced not only by the Kolmogorov length scale, but also by an appropriate thickness scale of the flame, for which, the locally thickened preheat zone thickness seems to be a good choice.

Formulation

The dissipation rate of turbulence energy ϵ. ϵ is often estimated by $\epsilon = A_0 u'^3/L_f$, where A_0 is a constant of order one (15). In this work, ϵ is based on the results obtained from the energy spectrum(10), and can be estimated by

$$\epsilon = A_1(u'^3/L_f)(\eta_K/L_f) \tag{10}$$

where A_1 is a constant of 11(14).

The Kolmogorov length scale η_K. From Eq.(10) and the definition of η_K, we have

$$\eta_K = L_f/(A_1^{0.2}\,Re^{0.6}) \tag{11}$$

The Taylor microscale λ_g. For the isotropic turbulence, λ_g can be calculated by(15)

$$\epsilon = 15\nu u'^2/\lambda_g^2 \tag{12}$$

thus, $$\lambda_g = \sqrt{15}L_f/(A_1^{0.4}Re^{0.2}) \tag{13}$$

The Karlovitz number Ka. According to the definition of η_0, $\eta_0 = \nu/(PrS_{L0})$. Substitution of Eqs.(11) and (13) into Eq.(7) yields

$$Ka = (Pr/\sqrt{15})(\eta_0/\eta_K)^2 \tag{14}$$

The wrinkled flame front burning velocity Sw. As all flamelets in the turbulent flame are assumed to have an inner cutoff of ϵ_i and an outer cutoff of ϵ_0, after the reasoning of Gouldin(9), the flame speed Sw as shown in Fig.10 can be estimated by

$$Sw = Sc = S_L(\epsilon_0/\epsilon_i)^{D_3-2} \tag{15}$$

where S_L is the local laminar burning velocity, and D_3 is the fractal dimension.

The fractal dimension D_3. Based on the measured results of the fractal dimension obtained from the flames of stoichiometric mixtures by Mantzaras et al(8), the fractal dimension D_3 is approximated by

$$D_3 = 2 + 0.5\exp\left\{\frac{-0.53}{\log(u'/S_{L0}+1)}\right\} \tag{16}$$

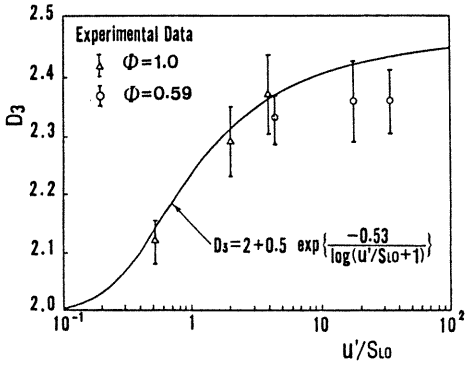

Fig.11 Comparison of Eq.(16) with experimental data(8)

The values of D_3 calculated by Eq.(16) are plotted in Fig.11 and compared with the measured results of reference (8).

The turbulent burning velocity S_T. As both the wrinkled flame front and the island flamelets are assumed to exist in the turbulent flame zone, S_T is then composed of the burning velocities of these two parts. Consider, for a unit area, during an infinitesimal time dt, the quantity of mixture consumed by the flame front, dFw, and that by the island flamelets, dF_D, are,

$$dFw = B(fw/\tau_C)dt, \quad dF_D = B(f_D/\tau_D)dt, \tag{17}$$

respectively, where B is a constant, being a characteristic thickness of the turbulent flame zone. This thickness is analogous to $2\delta_{L0}$ for a laminar flame and different from that defined in Fig.6. The total quantity of mixture consumed for a unit area is $dFw+dF_D$, thus,

$$\begin{aligned} S_T &= dFw/dt + dF_D/dt \\ &= B(fw/\tau_C + f_D/\tau_D) \\ &= B/\tau_T \end{aligned} \tag{18}$$

where $\tau_T = 1/(fw/\tau_C + f_D/\tau_D)$ is a characteristic time for the turbulent flame, analogous to τ_C for a laminar flame. As the burning velocity of the wrinkled flame front equals Sw, we have

$$Sw = B(fw/\tau_C), \tag{19}$$

$$B = Sw(\tau_C/fw) \tag{20}$$

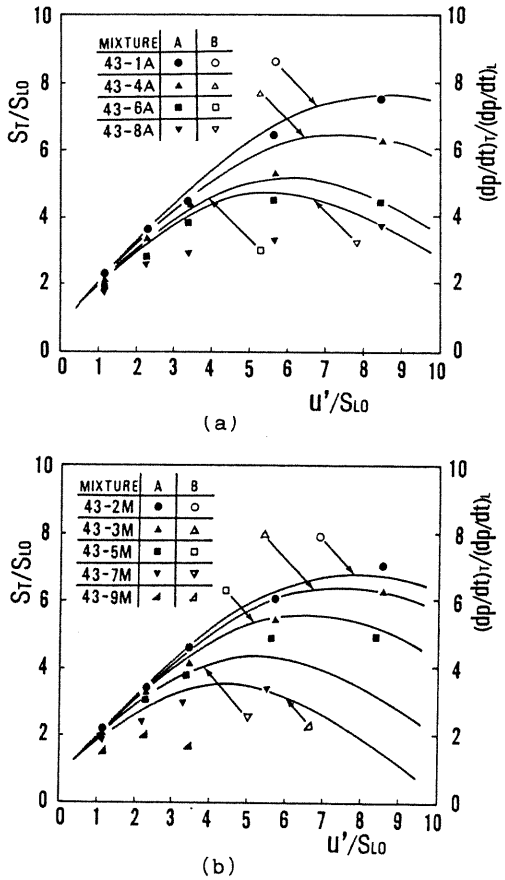

Fig.12 Comparison of model predictions with experimental data(16)
A-Experimental data; B-Model predictions

Prediction results and Discussion

In the above model, there are two constants involved: constant C in Eq.(4) and C_1 in Eq.(8). As the mass burning ratio S_T/S_{LO} can be approximated by the ratio of $(dp/dt)_T/(dp/dt)_L$, the two constant were such determined that the predicted S_T/S_{LO} ratio fitted the measured $(dp/dt)_T/(dp/dt)_L$ ratios most for mixture 43-1A(16), where dp/dt is the rate of pressure rise, subscripts T and L refer to turbulent flame and laminar flame, respectively. In this way, C=4.5 and C_1=0.5 were determined. Although there are two empirical constants involved in this model, if one assigns zero to both of them and 2.37 to D_3, this model is reduced into Gouldin's model logically.

Some of the predicted S_T/S_{LO} ratios for mixtures with different properties are given in Fig.12, showing that they are in good agreement with the measured $(dp/dt)_T/(dp/dt)_L$ ratios for most of the mixtures. But, for those mixtures which have extremely large laminar flame thicknesses such as mixtures 43-8A and 43-9M, the predicted values are too large. As such mixtures are usually not used in the real engines, the model is considered acceptable for practical use.

With this model, the flame zone thickness and the characteristic time of a turbulent flame can be calculated. The characteristic time is analogous to the transition time of $2\delta_{LO}/S_{LO}$, and so is the turbulent flame zone thickness to the thickness of $2\delta_{LO}$, for a laminar flame. The characteristic time and the characteristic flame zone thickness have been calculated and given in Fig.13, showing that the characteristic time is close to τ_C over a wide range of the u'/S_{LO} ratio, but the characteristic thickness increases with increasing u'/S_{LO} ratio.

CONCLUSIONS

1. Experiment results imply the structure of premixed propagating turbulent flames changing from a wrinkled single flamelet at low u'/S_{LO} ratios to an islands-like pattern at high u'/S_{LO} ratios.

2. The turbulent flame zone thickness increases with increasing the turbulence intensity for the same mixture, and decreases with increasing the laminar burning velocity, for different mixtures at the same turbulence intensity.

3. The separation distance between two successive flamelets in the flame zone is of the order of two times the turbulence longitudinal integral scale for three mixtures measured in this work.

4. The turbulent flame structure model proposed in this work can not only predict the S_T/S_{LO} ratios with appropriate accuracy for most of the mixtures except some with extreme properties, but also provide the characteristic thickness and the characteristic time of the turbulent flame.

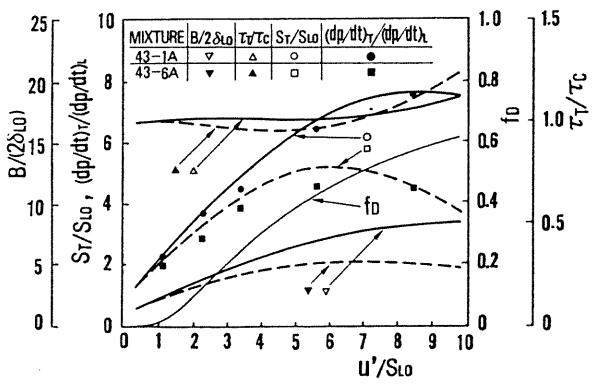

Fig.13 Model predicted influences of mixture properties on the turbulent flame
43-1A: S_{LO}=0.43m/s, η_0=0.0465mm, δ_{LO}=0.227mm
43-6A: S_{LO}=0.43m/s, η_0=0.0752mm, δ_{LO}=0.338mm(16)

REFERENCES

1. Kido,H., Huang,S.,and Nakashima,K., "A Study on the Structure of Premixed Propagating Turbulent Flames—An Investigation and Application of the Flame Plasma Potential Signals," Trans. Jpn Soc. Mech. Eng., Vol.56,No.521,pp.175-181,1990.
2. Libby, P.A. and Bray, K.N.C., "Implications of the Laminar Flamelet Model in Premixed Turbulent Combustion," Combust. Flame, Vol.39,pp.33-41, 1980.
3. Rajan, S., Smith, J. R., and Rambach, G. D., "Internal Structure of a Turbulent Premixed Flame Using Rayleigh Scattering," Combust. Flame, Vol.57, pp.95-107, 1984.
4. Kido,H., Huang,S.,and Nakashima,K., "A Study on the Fine-Structure of Propagating Turbulent Flames in Premixed Mixtures—An Analysis of the Schlieren Images Based on a Flame Structure Model," accepted to appear in Int. J. JSME.
5. Smith, J. R., "Turbulent Flame Structure in a Homogeneous-Charge Engine," SAE Trans. Vol.91, Sec.1, pp.150-164, 1982.
6. Baritaud,T.A. and Green,R.M.,"A 2-D Flame Visualization Technique Applied to the I.C. Engine," SAE Trans. Vol.95, Sec.1,pp.1.197-1.204, 1986.
7. Mantzaras, J., Felton, P.G., and Bracco, F. V., "Three-Dimensional Visualization of Premixed-Charge Engine Flames: Islands of Reactants and Products; Fractal Dimensions; and Homogeneity," SAE Paper, No. 881635, 1988.
8. Mantzaras, J., Felton, P.G., and Bracco, F. V., "Fractals and Turbulent Premixed Engine Flames,"Combust. Flame,Vol.77,pp.295-310,1989.
9. Gouldin F. C., "An Application of Fractals to Modeling Premixed Turbulent Flames," Combust. Flame, Vol.68, pp.249-266, 1987.
10. Kido, H., Wakuri, Y., Nakashima, K., and Hatanaka, K., "Flow Field Determination in Nearly Isotropic Turbulence of any Intensity by Hot-Wire Anemometry," Bull. JSME, Vol.24, No.187, pp.175-182, 1981.
11. Abraham, J., Williams, F.A., and Bracco, F.V., "A Discussion of Turbulent Flame Structure in Premixed Charges," SAE Paper, No.850345, 1985.
12. Peters, N., "Length and Time Scales in Turbulent Combustion," Turbulent Reactive Flows, (Borghi, R. and Murthy, S. N. B. Eds.), Springer-Verlag, pp.242-256, 1989.
13. Kido, H., Huang, S., and Nakashima, K., "Influences of Reynolds Number and Damkohler Number on the Structure of Premixed Turbulent Flames," Proc. 27th (Japanese) Symp. on Combust., pp.380-382, 1989.
14. Kido,H., Kitagawa,T.,Nakashima,K.,and Kato,K., "An Improved Model of Turbulent Mass Burning Velocity," Memories of the Faculty of Engrg., Kyushu Univ., Vol.49, No.4, pp.229-247, 1989.
15. Tennekes, H. and Lumley, J. L., A First Course in Turbulence, MIT Press, pp.67, 1972.
16. Kido, H., Wakuri,Y.,and Nakashima,K., "Experiment and Correlation of Turbulent Burning Velocity," Proc. ASME-JSME Therm. Engrg. Joint Conf., Vol.4, pp.183-190, 1983.